

See discussions, stats, and author profiles for this publication at: <https://www.researchgate.net/publication/261707367>

# Donor–Acceptor Polymers for Electrochemical Supercapacitors: Synthesis, Testing, and Theory

ARTICLE *in* THE JOURNAL OF PHYSICAL CHEMISTRY C · APRIL 2014

Impact Factor: 4.77 · DOI: 10.1021/jp5016214

---

CITATIONS

6

READS

80

---

## 5 AUTHORS, INCLUDING:



[Paul M DiCarmine](#)

University of Toronto

13 PUBLICATIONS 155 CITATIONS

[SEE PROFILE](#)



[Tyler B Schon](#)

University of Toronto

9 PUBLICATIONS 40 CITATIONS

[SEE PROFILE](#)



[Theresa M McCormick](#)

Portland State University

27 PUBLICATIONS 1,190 CITATIONS

[SEE PROFILE](#)



[Dwight Seferos](#)

University of Toronto

88 PUBLICATIONS 3,716 CITATIONS

[SEE PROFILE](#)

# Donor–Acceptor Polymers for Electrochemical Supercapacitors: Synthesis, Testing, and Theory

Paul M. DiCarmine,<sup>†</sup> Tyler B. Schon,<sup>†</sup> Theresa M. McCormick,<sup>†,§</sup> Philipp P. Klein,<sup>‡</sup> and Dwight S. Seferos\*,<sup>†</sup>

<sup>†</sup>Lash Miller Chemical Laboratories, Department of Chemistry, University of Toronto, 80 St. George Street, Toronto, Ontario M5S 3H6, Canada

<sup>‡</sup>Department of Chemistry, Johannes-Gutenberg Universität, Duesbergweg 10–14, 55099 Mainz, Germany

## Supporting Information

**ABSTRACT:** Donor–acceptor polymers can store both a positive and negative charge allowing them to function as both the positive and negative charge storage material in a supercapacitor device, however few have been explored for this application. Here, we describe the synthesis of several donor–acceptor polymers and their electrodeposited polymer electrodes. We use differing molecular structures to examine the effect of electron acceptor concentration and show that device stability can be improved significantly by increasing the acceptor concentration. Further, we provide computational insight into the important chemical requirements for achieving even higher performance supercapacitors based on donor–acceptor conjugated polymers. Supercapacitor devices with specific energy and specific power as high as 11 Wh kg<sup>-1</sup> (at 0.5 A g<sup>-1</sup>) and 20 kW kg<sup>-1</sup> (at 50 A g<sup>-1</sup> with an energy of 3.6 Wh kg<sup>-1</sup>) are reported, which are some of the highest values achieved to date.



## 1. INTRODUCTION

Supercapacitors are devices that can store a significant amount of energy and can be charged relatively quickly. High surface area carbon (HSAC)<sup>1,2</sup> is receiving much attention as an energy storage material for supercapacitors,<sup>3,4</sup> particularly with the recent advancements made in mesoporous carbon,<sup>5,6</sup> carbon nanotube,<sup>7,8</sup> graphene-based devices,<sup>9–13</sup> and the availability of commercial products.<sup>14,15</sup> HSAC supercapacitors store energy electrostatically through double-layer capacitance. This charge-storage mechanism is physical and is non-Faradaic. (No formal oxidation or reduction takes place.) Because of this physical charge-storage mechanism, these devices can be charged and discharged very rapidly.

Conjugated polymers store charge electrostatically; however, they also exhibit Faradaic charge storage (formal chemical oxidation and reduction),<sup>1,2,16</sup> which is an important distinction from HSACs. This combination of non-Faradaic charge separation and Faradaic charging allows conjugated polymers to store more energy than HSAC.<sup>2–4</sup> Oxidation or reduction occurs in a similar manner as a battery; however, the reaction quotient, or the extent of the reaction, depends on the applied potential, and thus the materials are considered pseudocapacitive.<sup>2</sup>

Some of the better known pseudocapacitive conjugated polymers include polythiophenes such as poly(3,4-ethyl-enedioxythiophene) (PEDOT), polypyrrole, and polyani-line.<sup>17–19</sup> Recent work has focused on blending these polymers with carbon nanotubes<sup>8,20</sup> or graphene<sup>21</sup> as well as adding redox-active pendant groups to the polymers<sup>22,23</sup> to improve

performance. Controlling the nanostructure of the polymers using hard and soft templates to increase specific capacitance, energy, and power<sup>24–29</sup> is also an important area of research. However, all of the aforementioned polymers have early oxidation potentials and are only capable of positive (p-type) as opposed to negative (n-type) or ambipolar charging. This limits the operating voltage of the device to the positive charging voltage range of the polymer (typically 0.8 to 1.4 V). This is important because stored energy can be increased by increasing the operating voltage window because energy is proportional to the square of the operating voltage (eq 1, where  $E$  is energy and  $C$  is capacitance).

$$E = \frac{1}{2}CV^2 \quad (1)$$

The donor–acceptor design is extremely attractive for narrow band gap conjugated polymers because the redox properties of the donor and acceptor moieties can be chemically tuned.<sup>30–44</sup> These narrow band gap polymers are typical in certain organic electronic applications<sup>45–55</sup> but atypical in supercapacitor research. When fabricated into a Type III polymer-based supercapacitor (one that operates with one electrode oxidized and one electrode reduced), they can significantly increase the operating voltage by storing both positive and negative charge depending on the applied

Received: February 14, 2014

Revised: March 28, 2014

Published: April 1, 2014



potential.<sup>56</sup> Only a handful of polymers have been applied to Type III devices,<sup>56–63</sup> and to the best of our knowledge, there is only one example of an alternating donor–acceptor copolymer used in a Type III device configuration. In that important study, the device degraded relatively rapidly due to the instability of the polymer in the reduced form, although the polymer was very stable under positive bias.<sup>64</sup> Previous work has shown that p-type polymers can be used in Type III devices when a large negative potential is applied. Despite larger bias, these previous studies report better cycle stability than D–A polymers.

We have designed a series of donor–acceptor polymers, characterized their electrochemical properties, synthesized electroactive films, and fabricated Type III supercapacitors to gain fundamental insight into their electrochemical charge-storage ability. While positive-charge delocalization within donor–acceptor polymers is well established, negative charge delocalization is somewhat ambiguous.<sup>65</sup> Estrada et al. observe localization of the LUMO on the acceptor moiety and charge-pinning upon reduction.<sup>64</sup> We explore the use of several EDOT-acceptor polymers and demonstrate that certain designs of electron-accepting units can improve negative charge delocalization, negative charge capacity, and the performance of D–A polymers in a Type III device.

## 2. EXPERIMENTAL SECTION

**General Considerations.** Reagents were purchased from Sigma-Aldrich and used as received unless otherwise noted. THF, DMF, dichloromethane, and acetonitrile were purified and dried using an Innovative Technology Pure Solv system. All electrochemical experiments were performed in an Innovative Technology Pure Lab nitrogen-filled glovebox using a BioLogic SP-200 potentiostat. Acetonitrile and dichloromethane used for electrochemistry were stored over molecular sieves in the glovebox. 2-(Tributylstanny)-3,4-(ethylenedioxy)thiophene was prepared according to a literature procedure.<sup>66</sup>

**Synthesis.** *5,8-Bis(2,3-dihydrothieno[3,4-b][1,4]dioxin-5-yl)quinoxaline (DEQ). Stille-Type Coupling Procedure (Adapted from Durmus et al.<sup>67</sup>)*. 5,8-Dibromoquinoxaline (0.513 g, 1.78 mmol) was added to a dry three-necked flask fitted with a condenser, a rubber septum, and a glass plug, under a nitrogen atmosphere. Anhydrous THF (100 mL) and 2-(tributylstanny)-3,4-(ethylenedioxy)thiophene (2.3 g, 5.3 mmol) were added to the flask. The solution was deoxygenated with bubbling nitrogen for 30 min.  $PdCl_2(PPh_3)_2$  (0.118 g, 0.176 mmol) was suspended in a small amount of THF and added to the reaction mixture by a syringe. The mixture was heated to reflux for 36 h, where it turned from light yellow to dark orange/red as the reaction proceeded. The mixture was allowed to cool, and the solvent was removed under vacuum to yield a red solid. Column chromatography on silica gel (3:1 dichloromethane/hexanes) afforded the desired product, a bright orange solid (0.240 g, 33%).

**Direct Heteroarylation Method.** A 10 mL Schlenk flask was flame-dried under vacuum and backfilled with nitrogen three times. 5,8-Dibromoquinoxaline (0.432 g, 1.50 mmol), palladium(II) acetate (0.034 g, 0.15 mmol), pivalic acid (0.046 g, 0.45 mmol), and potassium carbonate (0.621 g, 4.5 mmol) were added to the flask under a nitrogen atmosphere. DMA (3 mL) and 3,4-(ethylenedioxy)thiophene (0.80 mL, 7.5 mmol) were added to the flask by syringe. The mixture darkened quickly, and an orange solid appeared. The mixture

was allowed to stir at 100 °C for 70 min and then left to cool to room temperature. The mixture was diluted with dichloromethane, washed with water (three times) and brine, and the organic phase was separated, dried over  $MgSO_4$ , and filtered. The solvent was evaporated to yield the crude product, which was subsequently purified by column chromatography on silica gel (dichloromethane) to yield a bright-orange solid (0.268 g, 44%).  $^1H$  NMR (400 MHz,  $CDCl_3$ ,  $\delta$ ): 8.94 (s, 2H), 8.57 (s, 2H), 6.56 (s, 2H), 4.39–4.29 (m, 8H). HRMS (DART)  $m/z$ : [M + H]<sup>+</sup> calcd for  $C_{20}H_{15}N_2O_4S_2$ , 411.04732; found, 411.04746.

*2-(2,3-Dihydrothieno[3,4-b][1,4]dioxin-5-yl)-4,4,5,5-tetramethyl-1,3,2-dioxaborolane (1).* Synthesized as previously reported.<sup>68</sup>  $^1H$  NMR (400 MHz,  $CDCl_3$ ,  $\delta$ ): 6.62 (s, 1H), 4.35–4.13 (m, 4H), 1.34 (s, 12H).

*5-Bromo-8-(2,3-dihydrothieno[3,4-b][1,4]dioxin-5-yl)-quinoxaline (2).* 5,8-Dibromoquinoxaline (1.00 g, 3.47 mmol) and **1** (1.33 g, 3.47 mmol) were added to a flame-dried, 250 mL three-necked flask equipped with a condenser under an argon atmosphere. Toluene (140 mL) and water (8 mL) were added, and the solution was degassed by three freeze–pump–thaw cycles. Potassium carbonate (1.08 g, 7.81 mmol), tetrakis(triphenylphosphine)palladium(0) (0.200 g, 0.173 mmol), and Aliquat 336 (0.4 mL) were added to the flask, and the reaction mixture was allowed to stir at 84 °C for 64 h. The solution was diluted with dichloromethane and washed with water three times. The aqueous phase was extracted with dichloromethane. The combined organic phases were washed with brine, dried over magnesium sulfate, filtered, and concentrated. The crude product was purified by column chromatography on silica gel (dichloromethane) to yield the title compound (0.105 g, 9% yield).  $^1H$  NMR (400 MHz,  $CDCl_3$ ,  $\delta$ ): 8.99 (d,  $J$  = 1.8 Hz, 1H), 8.94 (d,  $J$  = 1.7 Hz, 1H), 8.44 (d,  $J$  = 8.3 Hz, 1H), 8.10 (d,  $J$  = 8.3 Hz, 1H), 6.59 (s, 1H), 4.40–4.28 (m, 4H), HRMS (DART)  $m/z$ : [M + H]<sup>+</sup> calcd for  $C_{14}H_{10}Br_1N_2O_2S_1$ , 348.96464; found, 348.96579.

*8,8'-Bis(2,3-dihydrothieno[3,4-b][1,4]dioxin-5-yl)-5,5'-biquinoxaline (DEDQ).* Potassium carbonate (0.081 g, 0.59 mmol) and **2** (0.068 g, 0.20 mmol) were added to a flame-dried 10 mL Schlenk flask under an nitrogen atmosphere. The flask was transferred to a nitrogen-filled glovebox, and 1,1'-bis(diphenylphosphino)ferrocene-palladium(II)dichloride (0.0044 g, 0.006 mmol) and bis(pinacolato)diboron (0.027 g, 0.11 mmol) were added to the flask. The flask was removed from the glovebox, and dry DMF (1.2 mL) was added. The mixture was stirred at 90 °C for 26 h, cooled to room temperature, and diluted with methanol, and the solids were collected on a glass frit. The solids were washed with methanol, followed by water, allowed to dry on the frit, collected, suspended in dichloromethane, and washed by three centrifugation/resuspension cycles to yield the title compound (0.027 g, 52%).  $^1H$  NMR (500 MHz,  $CD_2Cl_2$ ,  $\delta$ ): 8.87 (d,  $J$  = 1.6 Hz, 2H), 8.69 (d,  $J$  = 1.6 Hz, 2H), 8.66 (d,  $J$  = 7.7 Hz, 2H), 7.91 (d,  $J$  = 7.7 Hz, 2H), 6.59 (s, 2H), 4.43–4.30 (m, 8H). HRMS (DART)  $m/z$ : [M + H]<sup>+</sup> calcd for  $C_{28}H_{19}N_4O_4S_2$ , 539.08477; found, 539.08347.

*2-(3,4-Dimethoxythiophen-2-yl)-4,4,5,5-tetramethyl-1,3,2-dioxaborolane (3).* **3** was prepared in an analogous manner as **1** using 3,4-dimethoxythiophene (4.975 g, 34.50 mmol) to give a mixture of 3,4-dimethoxythiophene and the title compound (10 g, 89% crude yield), which was used in the next step without further purification.  $^1H$  NMR (400 MHz,  $CDCl_3$ ,  $\delta$ ): 6.46 (s, 1H), 4.00 (s, 3H), 3.82 (s, 3H), 1.31 (s, 12H).  $^{13}C$

NMR (100 MHz,  $\text{CDCl}_3$ ,  $\delta$ ): 154.62, 150.58, 147.82, 103.27, 96.29, 83.97, 61.34, 57.72, 24.66. HRMS (DART)  $m/z$ : [M + H]<sup>+</sup> calcd for  $\text{C}_{12}\text{H}_{20}\text{B}_1\text{O}_4\text{S}_1$ , 217.11753; found, 217.11666.

**5-Bromo-8-(3,4-dimethoxythiophen-2-yl)quinoxaline (4).** 4 was prepared in an analogous manner as 2 using 3 (0.619 g, 2.29 mmol) and excess 5,8-dibromoquinoxaline (1.980 g, 6.876 mmol). Column chromatography on silica gel (dichloromethane) allowed for the recovery of the excess 5,8-dibromoquinoxaline and isolation of the title compound (0.416 g, 52%). <sup>1</sup>H NMR (400 MHz,  $\text{CDCl}_3$ ,  $\delta$ ): 8.99 (d,  $J$  = 1.7 Hz, 1H), 8.95 (d,  $J$  = 1.8 Hz, 1H), 8.19 (d,  $J$  = 8.1 Hz, 1H), 8.14 (d, 1H), 6.42 (s, 1H), 3.91 (s, 3H), 3.79 (s, 3H). <sup>13</sup>C NMR (101 MHz,  $\text{CDCl}_3$ ,  $\delta$ ): 150.65, 145.69, 145.28, 144.41, 141.70, 140.85, 133.66, 132.36, 130.90, 123.06, 119.30, 98.80, 60.36, 57.43. HRMS (DART)  $m/z$ : [M + H]<sup>+</sup> calcd for  $\text{C}_{14}\text{H}_{12}\text{Br}_1\text{N}_2\text{O}_2\text{S}_1$ , 350.98029; found, 350.97989.

**8,8'-Bis(3,4-dimethoxythiophen-2-yl)-5,5'-biquinoxaline (DDQ).** Prepared in an analogous manner to DEDQ using 4. The compound was purified by Soxhlet extraction (hexanes, dichloromethane) through a glass frit. The title compound was isolated by concentrating the dichloromethane extracts (0.340 g, 53%). <sup>1</sup>H NMR (400 MHz,  $\text{CDCl}_3$ ,  $\delta$ ): 8.91 (d,  $J$  = 1.7 Hz, 2H), 8.73 (d,  $J$  = 1.7 Hz, 2H), 8.41 (d,  $J$  = 7.6 Hz, 2H), 7.94 (d,  $J$  = 7.6 Hz, 2H), 6.44 (s, 2H), 3.94 (s, 6H), 3.88 (s, 6H). <sup>13</sup>C NMR (101 MHz,  $\text{CDCl}_3$ ,  $\delta$ ): 150.67, 145.52, 144.36, 143.75, 142.34, 140.85, 137.55, 132.52, 132.20, 130.28, 120.37, 98.40, 60.52, 57.42. HRMS (DART)  $m/z$ : [M + H]<sup>+</sup> calcd for  $\text{C}_{28}\text{H}_{23}\text{N}_4\text{O}_4\text{S}_2$ , 543.11607; found, 543.11697.

**4-Bromo-7-(3,4-dimethoxythiophen-2-yl)benzo[c][1,2,5]thiadiazole (5).** 5 was prepared in an analogous manner as 2 using 4,7-dibromobenzo[c][1,2,5]thiadiazole (0.979 g, 3.33 mmol) and 3 (1.00 g, 3.33 mmol). Column chromatography on silica gel (dichloromethane:hexanes 8:2) followed by trituration with methanol afforded the title compound (0.262 g, 22%). <sup>1</sup>H NMR (600 MHz,  $\text{CDCl}_3$ ,  $\delta$ ): 8.17 (d,  $J$  = 7.8 Hz, 1H), 7.88 (d,  $J$  = 7.8 Hz, 1H), 6.44 (s, 1H), 3.91 (s, 3H), 3.89 (s, 3H). <sup>13</sup>C NMR (126 MHz,  $\text{CDCl}_3$ ,  $\delta$ ): 153.50, 152.34, 150.89, 132.50, 127.79, 125.76, 119.74, 112.14, 98.56, 60.12, 57.34. HRMS (DART)  $m/z$ : [M + H]<sup>+</sup> calcd for  $\text{C}_{12}\text{H}_{10}\text{Br}_1\text{N}_2\text{O}_2\text{S}_2$ , 356.93717; found, 356.93735.

**7,7'-Bis(3,4-dimethoxythiophen-2-yl)-4,4'-bibenzo[c][1,2,5]thiadiazole (DDDBT).** DDDBT was prepared in an analogous manner as DEDQ using 5. The product was purified by Soxhlet extraction (hexanes, dichloromethane) through a glass frit. The title compound was isolated by concentrating the dichloromethane extracts (0.219 g, 56%). <sup>1</sup>H NMR (500 MHz,  $\text{CDCl}_3$ ,  $\delta$ ): 8.50 (d,  $J$  = 7.7 Hz, 2H), 8.45 (d,  $J$  = 7.6 Hz, 2H), 6.46 (s, 2H), 3.96 (s, 6H), 3.94 (s, 6H). <sup>13</sup>C NMR (126 MHz,  $\text{CDCl}_3$ ,  $\delta$ ): 154.00, 153.39, 151.10, 145.91, 131.58, 128.22, 127.67, 126.22, 120.72, 98.62, 60.43, 57.50. HRMS (DART)  $m/z$ : [M + H]<sup>+</sup> calcd for  $\text{C}_{24}\text{H}_{19}\text{N}_4\text{O}_4\text{S}_4$ , 555.02891; found, 555.02843.

**2,5-Diphenyl-oxadiazole (DPODA).** DPODA was synthesized as previously reported.<sup>69</sup> <sup>1</sup>H NMR (400 MHz,  $\text{CDCl}_3$ ,  $\delta$ ): 8.18–8.13 (m, 4H), 7.61–7.48 (m, 6H). <sup>13</sup>C NMR (101 MHz,  $\text{CDCl}_3$ ,  $\delta$ ): 164.74, 131.86, 129.23, 127.09, 124.12. HRMS (DART)  $m/z$ : [M + H]<sup>+</sup> calcd for  $\text{C}_{14}\text{H}_{11}\text{N}_2\text{O}_1$ , 223.08714; found, 223.08756.

**Electrochemical Polymerization and Measurement.** Electrochemical polymerization was performed in a standard three-electrode electrochemical cell with a platinum disk working electrode (2 mm diameter), a platinum wire counter electrode, and a  $\text{Ag}/\text{Ag}^+$  reference electrode. The polymer-

ization solution contained 5 mM of the appropriate monomer and 0.1 M TBAPF<sub>6</sub> in dichloromethane. Deposition was stopped when the charge required to deposit a 5–10  $\mu\text{m}$  thick film had passed, ca. 30 cycles for the donor–acceptor monomers and 50 cycles for EDOT. Electrochemical measurements on polymer films were performed in a three-electrode cell in acetonitrile with 0.1 M TBAPF<sub>6</sub>. The ferrocene redox couple  $\text{Fc}^+/\text{Fc}$  has a half-wave potential of 0.09 V versus the reference electrode in the acetonitrile solution. Herein, the terms reduction and oxidation refer to the process of electron injection from the current collector to the polymer, and the process of electron injection from the polymer to the current collector, respectively.

**Polymer Electrolyte Preparation.** The polymer electrolyte was prepared in a nitrogen-filled glovebox by first making a solution of 1 M TBAPF<sub>6</sub> in acetonitrile. Poly(methyl methacrylate) (10% by weight; relative to the acetonitrile solvent) was added in small portions with stirring, waiting for each portion to fully dissolve before further addition. As the viscosity increased, the solution was heated slightly to facilitate polymer dissolution.

**Device Fabrication.** After electrochemical polymerization, polymer-coated electrodes were rinsed twice in dichloromethane and twice in acetonitrile. The electrodes were then immersed in a solution of 0.1 M TBAPF<sub>6</sub> and held at the midpoint of the operating voltage of the polymers versus  $\text{Ag}/\text{Ag}^+$  (0.30 V for PEDOT, −0.80 V for DEQ, and −0.51 V for PDDDBT) until the current decayed to zero (2 min). One electrode was inserted into a Teflon casing and coated with the electrolyte. An oven-dried paper circle cut from a Kimwipe was placed on top of the electrolyte-coated electrode. A second electrode was coated with the polymer electrolyte and pressed against the first within the Teflon casing with the paper separator held in between each electrode. The polymer electrolyte is viscous and will not leak from the device.

**Device Characterization.** The mass of the polymer films was estimated by the amount of charge passed during film formation. The total mass of both polymer electrodes was used to calculate specific energy and specific power. Energy was calculated by integrating the area under the discharge cycle of the charge–discharge curve and multiplying by the current density. Power was calculated by dividing the energy by the discharge time. Peak specific capacitance of the electrodes was determined by multiplying the current peak of the discharge CV scan of the device by the scan rate. (A correction factor 4 was used to account for the series connection and the mass difference between the device and a single electrode.) Electron microscopy was performed using a Quanta FEG 250 ESEM.

**Computational Methods.** The geometries of the oligomers 12 rings long of PEDOT, PDEQ, and PDDDBT as well as a block copolymer version of PDDDBT (EDOT-*b*-BT) were optimized with the nonlocal hybrid Becke three-parameter Lee–Yang–Parr<sup>70</sup> with Handy and coworkers’ long-range corrected version using the Coulomb-attenuating method (CAM-B3LYP)<sup>71</sup> functional and the 6-311g(d) basis set on the Gaussian 09 suit of programs.<sup>72,73</sup> The geometry of oxidized and reduced versions of each oligomer was optimized with the same basis set and level of theory (+1 doublet, −1 doublet). Coordinates for optimized geometries are listed in the Supporting Information. The frontier orbitals are visualized with an isocontour value of 0.03. Bond length change plots were made by taking difference of the optimized bond lengths of the neutral geometry and the oxidized or reduced

geometries. The plots show that the bond length change down the conjugated backbone is indicative of the changes seen if all bonds are considered.

### 3. RESULTS AND DISCUSSION

**3.1. Molecular Design.** We examine five donor–acceptor monomers: 5,8-bis(2,3-dihydrothieno[3,4-*b*][1,4]dioxin-5-yl)-quinoxaline (**DEQ**), 8,8'-bis(2,3-dihydrothieno[3,4-*b*][1,4]-dioxin-5-yl)-5,5'-biquinoxaline (**DEDQ**), 8,8'-bis(3,4-dimethoxythiophen-2-yl)-5,5'-biquinoxaline (**DDDQ**), 7,7'-bis(3,4-dimethoxythiophen-2-yl)-4,4'-bibenzoz[*c*][1,2,5]thiadiazole (**DDDBT**), 2,5-diphenyl-1,3,4-oxadiazole (**DPODA**), as well as 3,4-ethylenedioxythiophene (**EDOT**) (Figure 1). The mono-

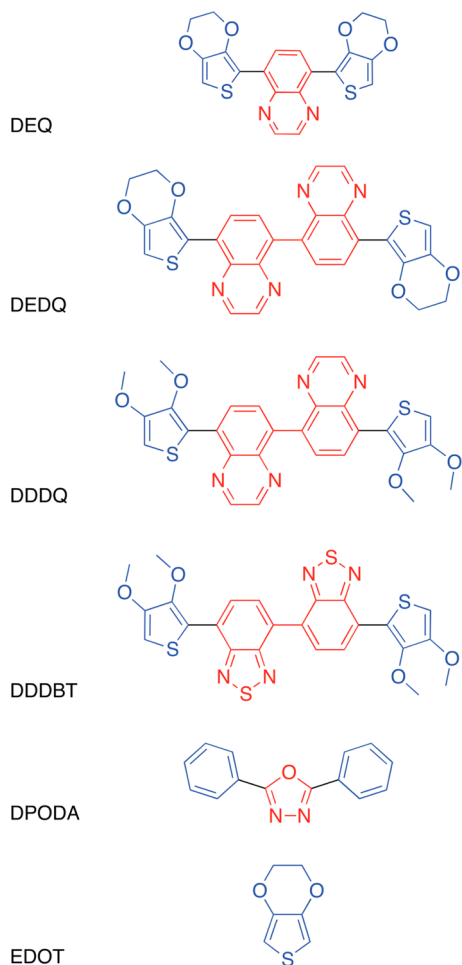


**Figure 1.** Structures of the monomers used in this study. Donor units are colored blue, and acceptor units are colored red.

mers were selected to study the effect of increasing the acceptor to donor ratio in the polymers (Chart S1 in the Supporting Information). Synthesis as well as three important molecular design factors are considered: solubility, film formation, and electrochemical potential range.

**3.1.1. Synthesis.** Donor–acceptor–donor (D-A-D) monomers with EDOT or other thiophene-like end groups, like DEQ, are important compounds for organic electrochromic applications<sup>65,67,74–79</sup> and more recently have been applied to photovoltaic,<sup>80–83</sup> field-effect transistor,<sup>84</sup> and sensing<sup>85</sup> applications. Most syntheses involve at least three steps, require an organolithium reagent, and include the preparation

of an organostannane reagent. The organostannane compounds, which are less desirable due to toxicity concerns, are used in excess (up to 2.5 times the stoichiometric requirement).<sup>67</sup> Here we use direct heteroarylation for the synthesis of a D-A-D monomer, eliminating the use of organolithium and organostannane reagents and the need for cryogens, and achieve yields comparable to Stille coupling with much higher atom economy. Direct heteroarylation is a one-step, one-pot reaction conducted at moderate temperature<sup>86–88</sup> (Figure 2). Although not the focus of this report, this technique is very straightforward and will be useful to others synthesizing similar D-A-D monomers.

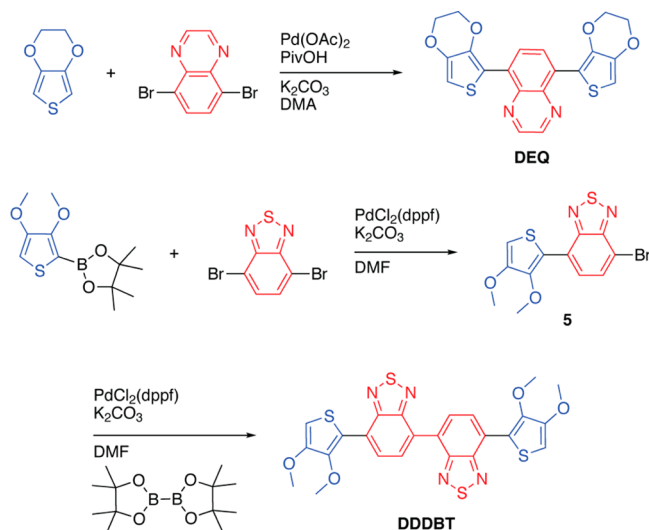


**Figure 2.** Synthesis of DEQ by direct heteroarylation and Suzuki-type synthesis of DDDBT. DEDQ and DDDQ were synthesized in a similar fashion to DDDBT.

The donor–acceptor monomers, DEDQ, DDDQ, and DDDBT, were synthesized using Suzuki–Miyamura coupling. First, EDOT or 3,4-dimethoxythiophene was treated with an organolithium reagent, followed by isopropoxyboronic acid pinacol ester to yield the corresponding boronic ester. The boronic ester was then treated with the dibrominated acceptor molecule (5,8-dibromoquinoxaline or 4,7-dibromobenzoz[3,4-*c*][1,2,5]thiadiazole) in a one-to-one ratio. The monobrominated product was then subjected to a one-pot in situ boronic esterification and coupling using half an equivalent of bis(pinacolato)diboron to generate the boronic ester in the presence of the bromo species, allowing for conventional Suzuki–Miyamura coupling.<sup>89</sup>

**3.1.2. Solubility and Solubilizing Side Chains.** Solubility is an important parameter for any solution-based approach to polymerization. Side chains increase the solubility of the monomer; however, alkyl side chains act as insulators and are not electrochemically active, and thus the side-chain size should be minimized. For electropolymerized materials, it is sufficient for the monomer to be soluble and not the corresponding oligomers/polymers, as deposition of insoluble oligomers/polymers is desired. No solubilizing groups are required for the D-A-D monomers; however, we found that the D-A-A-D monomer DEDQ was not suitably soluble to undergo electropolymerization from solution. Dimethoxythiophene has similar electronic properties to EDOT but has free rotation of the methoxy groups and more conformational degrees of

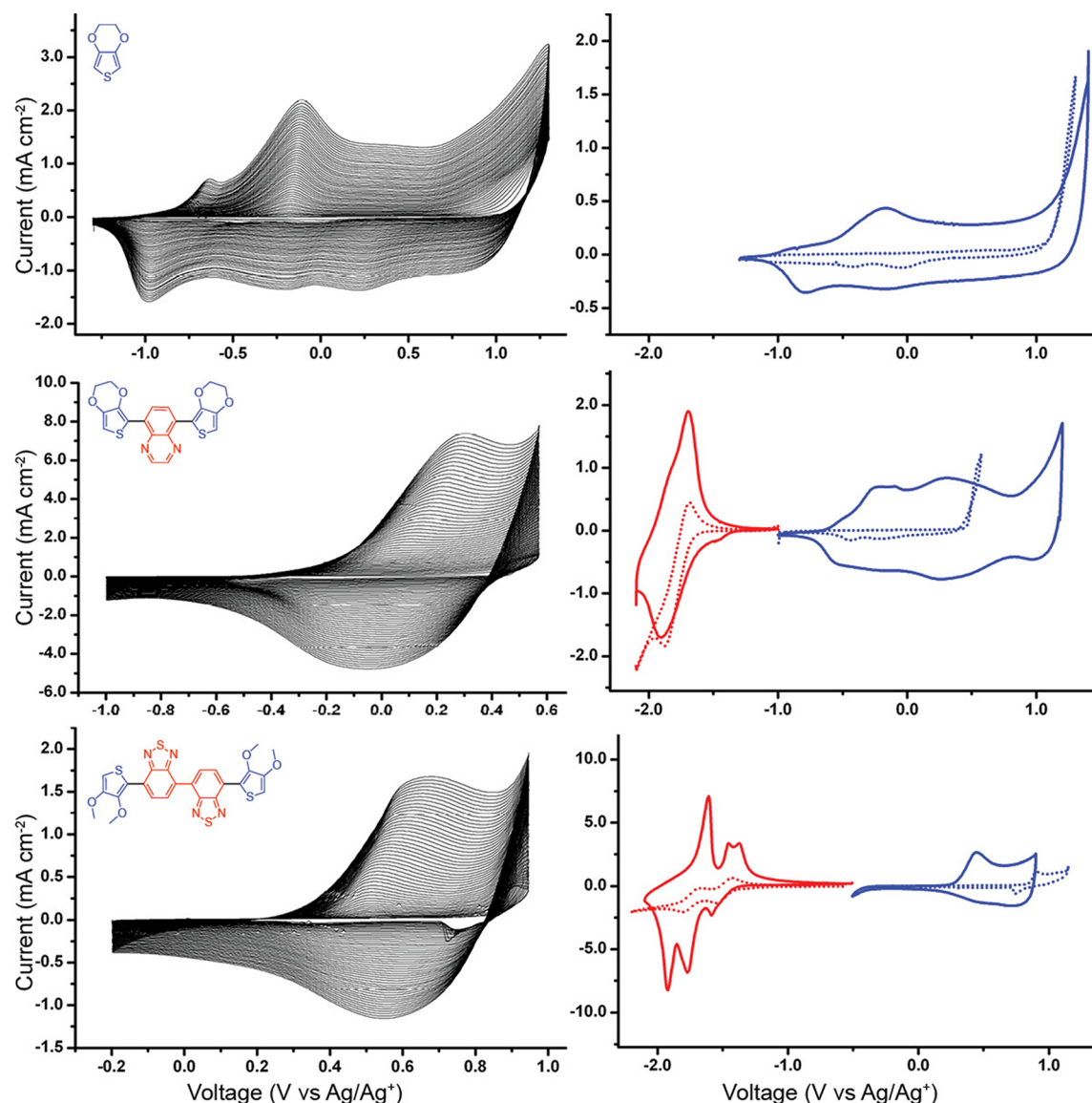


**Figure 3.** Left column: electrochemical polymerization and deposition of polymers by cyclic voltammetry (the corresponding monomer is inset). Right column: cyclic voltammograms of PEDOT, PDEQ, and PDDDBT films (solid lines) and the respective monomers (dotted lines).

freedom. Replacing EDOT with dimethoxythiophene in the DDDQ and DDDBT monomers increased the solubility significantly and allowed for the preparation of appropriately concentrated solutions (5 mM).

**3.1.3. Film Formation.** Electrochemical polymerization<sup>17,18,90</sup> affords several advantages for polymer film formation: polymers are formed directly on the electrode surface, and films several micrometers thick can be readily deposited. However, certain electronic factors will make electrochemical polymerization extremely challenging, and thus judicious selection of monomers is essential. For example, DPODA has a reversible reduction wave, as does the alternating poly(phenylene-*alt*-1,3,4-oxadiazole),<sup>91,92</sup> and appears to be a good candidate for an n-type polymer, it is synthesized in high yield, and the ionization energy is predicted to be  $-6.40 \text{ eV}$  by DFT, the same as 3-methylthiophene, which is readily electropolymerized.<sup>60</sup> However, we found that it cannot be polymerized electrochemically because the oxidation potential of the monomer is too high. DEQ and DDDBT are readily polymerized by cyclic voltammetry in an analogous

manner to EDOT (Figure 3), and several micrometer-thick films of oligomers/polymers are formed.

The cross sections of the PDEQ and PDDDBT films indicate that the morphologies of the two films are quite different (Figure 4). The PDEQ film is composed of small clusters of material with very small grain sizes. The PDDDBT film is composed of much larger domains of oligomer/polymer. This is likely due to faster grain nucleation for DEQ compared with DDDBT.

To our surprise, although structurally similar to DDDBT, DDDQ cannot be polymerized electrochemically. Irreversible oxidation is observed, but the peak fails to increase with subsequent oxidation scans (Figure S1 in the Supporting Information). A very thin film is observed on the electrode surface. Because the monomer is oxidized but only produces a very thin film, we hypothesize that the film is not suitably conductive for subsequent growth. This is likely the result of steric hindrance that leads to a large dihedral angle between adjacent quinoxaline groups and disrupts the conjugation along the molecule (Figure S2 in the Supporting Information). The

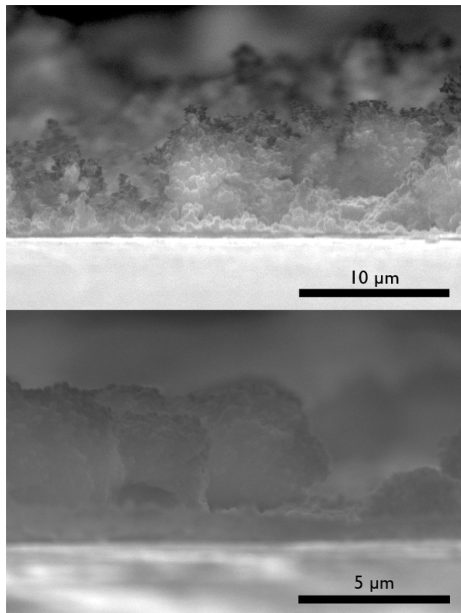


**Figure 4.** Scanning electron microscopy images of a cross-section of PDEQ (top) and PDDDBT (bottom) films. The platinum current collector appears light (at the bottom) and the polymer appears dark (in the middle) in each corresponding image.

predicted dihedral angle between the two quinoxalines in DDDQ is  $49.0^\circ$  (DFT calculation) compared with only  $31.2^\circ$  between the benzothiadiazoles in DDDBT. We focus on the three electropolymerizable monomers: EDOT, DEQ, and DDDBT.

**3.2. Capacitive Properties.** The electrochemical response of PEDOT, PDEQ, and PDDDBT was investigated using cyclic voltammetry in a standard three-electrode electrochemical cell (Figure 3, Chart S2 in the Supporting Information). Charge carrier delocalization and pseudocapacitance are important criteria for conjugated polymer supercapacitors. A shift of the oxidation onset (or reduction onset) to potentials of lower magnitude as the monomer is converted to the oligomer/polymer is indicative of delocalization, which is due to the formation of low energy states.

PEDOT has a wide, rectangular cyclic voltammogram, indicative of charge delocalization. Similarly, the cyclic voltammogram of PDEQ exhibits a broad flat current response at oxidative potentials, which indicates gradual positive charging over a relatively broad potential range. However, at reductive potentials, a much narrower peak is observed. Comparing the area of the oxidative wave to the reductive wave of PDEQ, it is apparent that the material can store more positive charge than negative charge. In contrast with a large stabilization of the HOMO energy level (ca. 750 mV), the reduction onset increases only slightly (ca. 20 mV), and thus there is very little LUMO stabilization upon polymerization. These observations

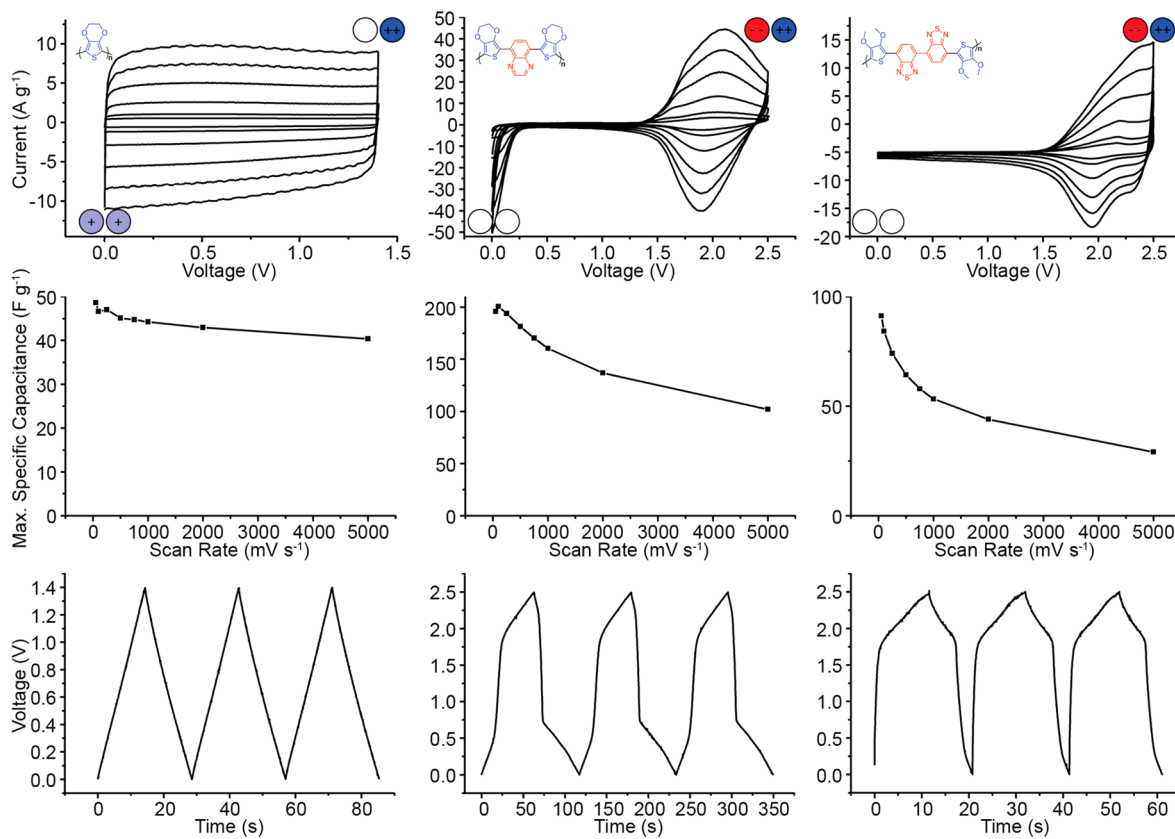


**Figure 5.** Electrochemical characterization of Type I PEDOT (left column), Type III PDEQ (middle column), and Type III PDDDBT devices (polymer structure inset in corresponding column). Top row: cyclic voltammetry at 50, 100, 200, 500, 750, and 1000  $\text{mV s}^{-1}$ . The electrodes where the electron donor material stores charge are in blue, where the electron acceptor stores charge are in red, and a neutral electrode is white. The state of charge on the electrode for the discharged and charged device is indicated by “+” and “−”. Middle row: peak capacitance versus scan rate. Bottom row: charge–discharge at  $1 \text{ A g}^{-1}$  current density.

indicate that there is good delocalization in the positively charged film but poor delocalization in the negatively charged film, and although PDEQ is reducible, it more closely resembles a redox couple than an ambipolar pseudocapacitative material.

PDDDBT was designed with two electron acceptor heterocycles to increase electron delocalization along the polymer backbone and to better match the amount of positive and negative capacitance of the material. The cyclic voltammogram of PDDDBT reveals several interesting results. First, the reduction onset of the DDDBT monomer is decreased in magnitude relative to DEQ. However, in contrast with a large stabilization (ca. 600 mV) of the HOMO energy level upon polymerization, there is almost no LUMO level stabilization. The dual acceptor units result in multiple reduction processes over a wide potential range.

Taken together, it is clear that the width of the positive charging range decreases with increasing acceptor concentration. For PEDOT, PDEQ, and PDDDBT, the positive charging range is 1400, 980, and 840 mV respectively. This reduces the capacitive contribution of the positive electroactive range to the device. However, introducing two acceptor moieties in PDDDBT allows for more negative charge to be accepted compared with PDEQ and causes the charge stored in the negative electroactive range to much better match the positive range. Finally, the voltage from the edge of the positive charging range to the edge of the negative charging range is 2.9 and 3.2 V for PDEQ and PDDDBT, respectively. This will equate to a device that has a higher operating voltage than PEDOT.

**3.3. Supercapacitors.** Supercapacitors composed of conjugated polymers are fabricated in four configurations, termed Types I–IV.<sup>19,56</sup> In this study, we focus on Type I and Type III supercapacitors, referred to as symmetric devices because both electrodes are composed of the same material. In a Type I device, both electrodes operate in either the positive or negative electrochemically active voltage range of the material but not both. Because p-type conjugated polymers are the most common, Type I conjugated polymer devices are most commonly operated by each electrode accepting and donating positive charges. In this configuration, the negative electrode operates in the lower half of the potential range, while the positive electrode operates in the higher half of the potential range. When the device is discharged, the chemical potential across the device is zero and both electrodes retain the same partial positive charge. When the device is charged, the positive electrode becomes fully positively charged and the negative electrode is neutral. The cell voltage of a Type I PEDOT device is limited to 1.4 V, the electrochemically active range of the polymer and the difference between the fully charged and fully discharged potential.

In a Type III device, the positive electrode operates by accepting and donating positive charges, while the negative electrode operates by accepting and donating negative charges. When the device is discharged, both electrodes are neutral and the cell voltage is zero. Charging the device causes the positive electrode to become positively charged and the negative electrode to be negatively charged. This cell voltage is higher than what can be achieved in a Type I device. These two different operating mechanisms are illustrated on the device cyclic voltammograms by the colored circles (Figure 5).

Type III supercapacitors were fabricated using PDEQ and PDDDBT as the charge storage material, and Type I devices were made using PEDOT to illustrate the differences in

electrode materials and device performance. In brief, each device was fabricated by polymerizing monomers using cyclic voltammetry on two platinum button electrodes. The electrodes were rinsed in monomer-free electrolyte solution. The cyclic voltammogram of the polymer in a three-electrode cell is used as a guide for conditioning the electrodes prior to device fabrication. First, the operating voltage of the device is determined (2.5 V for PDEQ and PDDDBT, 1.4 V for PEDOT); then, the electrodes are charged to the midpoint of the operating voltage range (−0.80, −0.51, and 0.30 V vs Ag/Ag<sup>+</sup> for the PDEQ, PDDDBT, and PEDOT devices, respectively). This allows for the best overlap of the electroactive range(s). The electrodes were then coated with a poly(methyl methacrylate)/tetrabutyl ammonium hexafluorophosphate/acetonitrile electrolyte. One electrode was placed into one end of a custom-made Teflon casing (Figure S3 in the Supporting Information), a porous paper disk separator was placed on top of the electrolyte-coated electrode, and the second electrode coated with polymer electrolyte was inserted to create a sandwich-type device.

The performance of the Type III PDEQ and PDDDBT devices were measured over 2.5 V, and the Type I PEDOT device was measured over 1.4 V (Figure 5). Devices were cycled at various scan rates (50 mV s<sup>−1</sup> to 5 V s<sup>−1</sup>). From the cyclic voltammogram, it is apparent that the Type III devices only exhibit pseudocapacitance at potentials above 1.5 V. However, because of the energy–voltage relationship (eq 1), 75% of the energy in a capacitor is stored in the highest 50% of the operating voltage. This is advantageous because the vast majority of the charge on the devices is extracted at potentials above 1.5 V. The current of the PDEQ device begins to diminish after 2.0 V, whereas the PDDDBT has a broader current profile up to 2.5 V. This is due to better capacitance matching of the negative and positive electrode. Peak capacitance measured from the discharge scan is plotted as a function of scan rate (Figure 5). The device electrodes exhibit excellent capacitance, even at scan rates as high as 5 V s<sup>−1</sup>, with a maximum value of 201 and 91 F g<sup>−1</sup> (obtained at 100 and 50 mV s<sup>−1</sup>) for the PDEQ and PDDDBT devices, respectively.

Charge–discharge measurements were performed on the devices at current densities of 0.2–50 A g<sup>−1</sup>. (The 1 A g<sup>−1</sup> measurements are presented.) The typical triangular charge–discharge curve is observed for the Type I PEDOT device. However, for both Type III devices, the shape is different due to the initial, fast, non-Faradaic charging at potentials too low for pseudocapacitance. This causes the potential of the Type III device to increase sharply, followed by a more gradual increase in potential as the pseudocapacitative charging of the electrodes takes place. Average capacitance for the electrodes was calculated from the discharge measurement at 0.5 A/g.<sup>93</sup> Measuring average capacitance over the entire voltage range (1.4 V for PEDOT and 2.5 V for PDEQ and PDDDBT) yields average specific capacitances of 41 F/g for PEDOT, 88 F/g for PDEQ, and 17 F/g for PDDDBT. Most supercapacitors are operated from  $V_{\max}$  to  $V_{1/2}$ <sup>93</sup> and using  $dV = V_{\max} - V_{1/2}$ , the average specific capacitance is 37 F/g for PEDOT, 30 F/g for PDEQ, and 25 F/g for PDDDBT. Finally, using  $dV = V_{\max} - V_{\text{pseudo}}$  where  $V_{\text{pseudo}}$  is the onset voltage of the pseudocapacitive region for the donor–acceptor polymers, gives a specific capacitance of 72 F/g for DEQ (over a range of only 0.3 V) and 40 F/g for PDDDBT (over a range of 0.675 V).

The PEDOT and PDDDBT devices are nearly symmetric upon charging/discharging; however, the PDEQ device is not.

The cycling efficiency, as measured by the difference in area of the charging and discharging curve (measured 1 A g<sup>-1</sup>), is 98% for PEDOT, 38% for PDEQ, and 60% for PDDDBT, again demonstrating that adjacent electron acceptors improve device performance. The longer charging time for the PDEQ device and rapid potential drop upon discharge are due to negative charge leakage.

The specific energy and power for the devices are extracted from the charge/discharge plots, and both exceed the specific energy of PEDOT (Figure 6, Table 1). The specific energy and

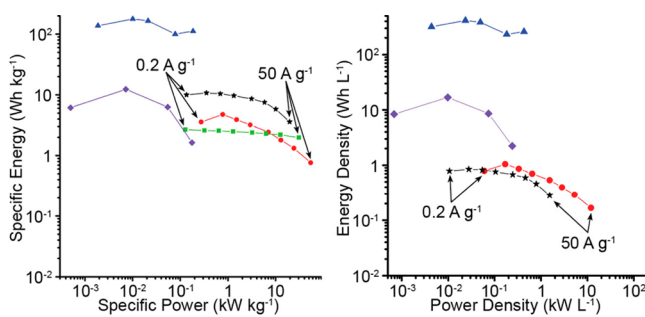


**Figure 6.** Ragone plots of PDEQ (black stars), PDDDBT (red circles), and PEDOT (green squares) devices compared with a commercial lithium ion battery (blue triangles) and a commercial double-layer supercapacitor (purple diamonds). The polymer devices were measured at 0.2, 0.5, 1.0, 2.0, 5.0, 10, 20, and 50 A g<sup>-1</sup>. Data points for the 0.2 and 50 A g<sup>-1</sup> measurements are labeled.

specific power of the PDEQ device are 11 Wh kg<sup>-1</sup> (at 0.5 A g<sup>-1</sup>) and 20 kW kg<sup>-1</sup> (at 50 A g<sup>-1</sup> with a specific energy of 3.6 Wh kg<sup>-1</sup>), respectively. The PDDDBT device has a specific energy of 4.8 Wh kg<sup>-1</sup> (at 0.5 A g<sup>-1</sup>) and a very high specific power of 55 kW kg<sup>-1</sup> (at 50 A g<sup>-1</sup> with a specific energy of 0.76 Wh kg<sup>-1</sup>), respectively. For ease of comparison with other published figures for new materials,<sup>21,94–97</sup> only the mass of the active material is considered in these calculations. The mass of the active layers was estimated by the charge passed during electrochemical deposition.<sup>96</sup> We assumed that the deposition is 100% efficient; however, the Coulombic efficiency of electrochemical polymerization can be as low as 16%,<sup>98,99</sup> which means that performance values are an underestimation of the true values. The volumetric performance is reported for the PDEQ and PDDDBT devices because their respective polymerization efficiencies are likely different. The energy and power density of the PDEQ device are 0.84 Wh L<sup>-1</sup> (at 0.5 A g<sup>-1</sup>) and 1.5 kW L<sup>-1</sup> (at 50 A g<sup>-1</sup> with an energy density of 0.28 Wh L<sup>-1</sup>), respectively. For the PDDDBT device, the values are 1.0 Wh L<sup>-1</sup> (at 0.5 A g<sup>-1</sup>) and 12 kW L<sup>-1</sup> (at 50 A g<sup>-1</sup> with an energy density of 0.16 Wh L<sup>-1</sup>), respectively. Thus, on a volumetric scale, PDDDBT performs slightly better than PDEQ.

**Table 1. Performance Metrics of the Supercapacitor Devices**

material	peak capacitance [F g <sup>-1</sup> ] <sup>a</sup>	specific energy [Wh kg <sup>-1</sup> ] <sup>b</sup>	specific power [kW kg <sup>-1</sup> ] <sup>c</sup>	energy density [Wh L <sup>-1</sup> ] <sup>d</sup>	power density [kW L <sup>-1</sup> ] <sup>d</sup>
PEDOT	49	2.8	31		
PDEQ	201	11	20	0.84	1.5
PDDDBT	91	4.8	55	1.0	12

<sup>a</sup>Peak capacitance of an individual electrode. <sup>b</sup>Specific energy calculated by integrating the area under the discharge curve multiplying by the current density (at 0.5 A g<sup>-1</sup>). <sup>c</sup>Specific power was calculated by dividing the specific energy by discharge time (at 50 A g<sup>-1</sup>). <sup>d</sup>Energy and power density values were calculated by measuring the thickness of the polymer layer from electron microscopy images and the area of the electrode.

Although higher energy values have been reported for electrodeposited polymer Type III supercapacitors, ranging from 6–53 Wh kg<sup>-1</sup>,<sup>56,58,59,61</sup> most use highly porous carbon fabric as the current collector and are measured in a flooded cell rather than as an assembled device. Improved specific energy and very high specific power can be achieved by nanostructuring the polymer.<sup>25</sup>

Cycle stability measurements were performed on the supercapacitor devices (Figure 7). PEDOT is well known to

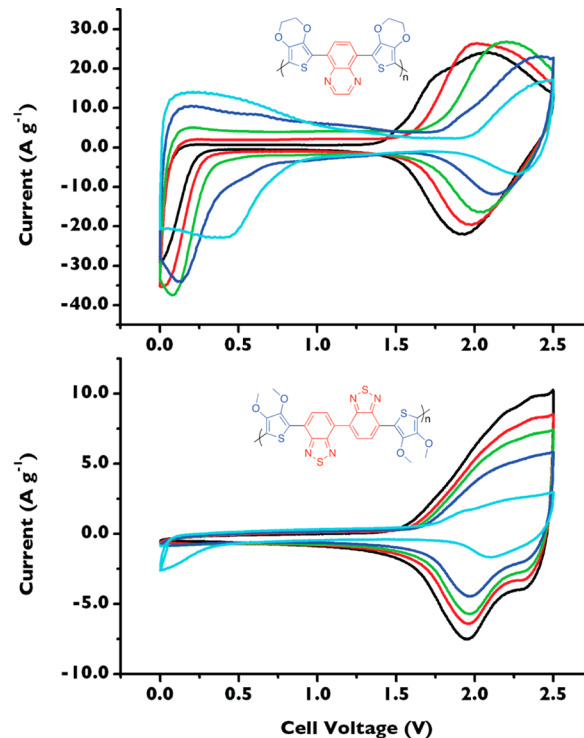


**Figure 7.** Cyclic voltammograms of a PDEQ (top) and PDDDBT supercapacitors at 500 mV s<sup>-1</sup>. Cycles 2, 50, 100, 250, and 1000 shown.

be highly stable and does not significantly degrade after 1000 cycles at 1.4 V (Figure S4 in the Supporting Information). The multicycle CV of PDEQ illustrates the importance of good negative charging stability. The pseudocapacitive peak of the PDEQ capacitor shifts to higher potentials with increasing scan number, while a low voltage peak begins to appear. This effect is due to current leakage from the negative electrode. Initially, when the device is at 0 V, each electrode is at -0.80 V versus Ag/Ag<sup>+</sup>, a conditioning voltage in the middle of the band gap. When the device is scanned, the positive electrode collects and holds positive charge, and the negative electrode collects an equivalent amount of negative charge; however, some of this charge leaks and the negative electrode never achieves a full

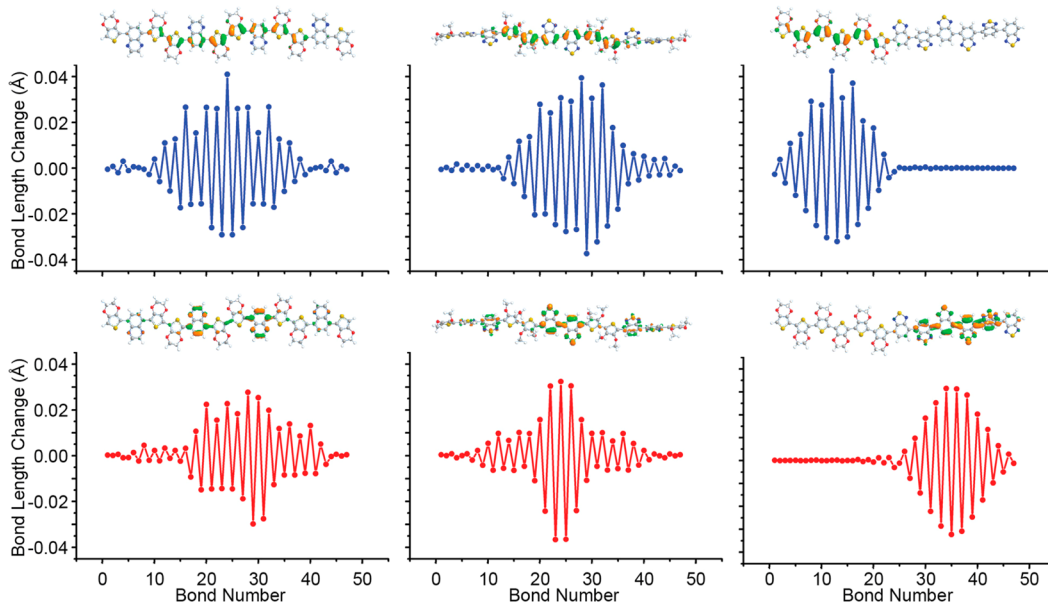


**Figure 8.** Change in bond length along the acetylene backbone from neutral to +1 (blue, top row) and neutral to −1 (red, bottom row) doublet states for PDEQ, PDDDBT, and P(EDOT-*b*-BT) models (left to right). The orbital diagrams of the HOMO and LUMO of the neutral polymer are above the neutral minus +1 and neutral minus −1 plots, respectively.

charge. Over multiple scans, the 0 V point drifts out of the band gap into the positive charging range of the electrodes. Eventually the device acts as a Type I capacitor from 0 to ca. 0.75 V and then a Type III capacitor from 2 to 2.5 V.

Installing a second acceptor unit in the polymer backbone allows better charge stabilization and prevents significant charge leakage. Peak shifting due to charge leakage is not seen in the PDDDBT device. Although the performance of the device itself does diminish with cycling, it maintains 75% initial capacity after the first 100 cycles and 30% of initial capacity after 1000 cycles. Estrada et al. reported an electrodeposited Type III device based on poly(bis-EDOT-isoindigo) films prepared on gold electrodes that achieve 15 Wh kg<sup>−1</sup>, which was fully degraded after 200 cycles.<sup>64</sup> When compared with a Type I supercapacitor, the stability is not impressive; however, it is clear that in Type III device configuration adjacent acceptor units improve the cyclability. Type III devices are very distinct from Type I devices because the polymer must accept both a positive and negative charge, a much more challenging materials design requirement. Materials development for Type III devices is imperative to achieve stable operation above 1 to 1.4 V, which increases energy and power densities. In contrast with the hundreds of papers on donor–acceptor polymers in photovoltaics, little is known about the performance of these materials in supercapacitors, and the wide variety of acceptor moieties available promise significant potential for improvement. This report represents an important step forward in the development and advancement of Type III supercapacitors. Although more improvement is required, this is the first time a Type III donor–acceptor supercapacitor has been shown to have stability beyond ~200 cycles.

The decrease in current with cycling is likely due to slow degradation of the polymer during reduction. It is possible that the reduced state can be further stabilized by blending the active polymer with an appropriate material to stabilize it through specific chemical interactions, as was recently demonstrated with a polyaniline/polyacid blend.<sup>100</sup> Mastragostino et al. reported an electrodeposited poly(3-methylthio-

phene) Type III device prepared on platinum that achieved an energy density of 13 Wh kg<sup>−1</sup>; however, stability was achieved only after the polymer was coated onto a stainless-steel grid electrode and blended with a binder and carbon black.<sup>60</sup> Similar methods are expected to improve the stability of the new polymers presented here but are beyond the scope of the present study.

**3.4. Theoretical Modeling.** Theoretical modeling provides important insight into the observed electrochemical differences and future materials design. Capacitance matching of the positive and negative charging ranges is important when designing materials for Type III supercapacitors. It is also important that there is charge delocalization in both the oxidized and reduced states of the polymer. The extent of charge delocalization across the polymers was examined using computational chemistry. Geometry optimizations (density functional theory)<sup>101</sup> of model oligomers with 12 aromatic moieties were performed using Gaussian 09<sup>72</sup> on PEDOT, PDEQ, and PDDDBT, as well as a hypothetical block copolymer version of PDDDBT (EDOT-*b*-BT; six monomers per block). Here we are interested in how the bond lengths along backbone of the polymer change in the +1 and −1 oxidation and reduction states relative to the neutral ground states. Smaller bond length changes (in the +1 or −1 state compared with the ground state) that are spread over several repeat units indicate that the charge (positive or negative) is also spread over multiple repeat units and thus indicates delocalization of the oxidized or reduced form. Larger bond length changes that are isolated indicate greater localization. For clarity, only the bond length changes within the acetylene backbone are shown (Figure 8). The calculated HOMO and LUMO orbital distributions for the neutral polymer are presented with the +1 and −1 bond length change plots, respectively.

For PEDOT, the bond length change in the +1 doublet state is spread over many repeat units (Figure S5 in the Supporting Information), which we interpret as a great deal of charge delocalization. The models for PDEQ and PDDDBT are more

localized in both the +1 and -1 states. It is apparent that the positive charge resides mostly on the electron rich heterocycles, whereas the negative charge resides on the electron-deficient heterocycles. This reinforces the hypothesis that delocalization of charge carriers in donor–acceptor copolymers is not as great as in homopolymers like PEDOT. Furthermore, on the basis of the model compounds, there is greater delocalization of the negative charge when the number of adjacent acceptors is increased, as predicted for PDDDBT. Considering all bond lengths but excluding those to hydrogen (Figures S6–S11 in the Supporting Information) shows identical trends.

We performed the same computational analysis on a hypothetical donor–acceptor block copolymer. Here the positive charge resides exclusively on the donor block, while the negative charge resides on the acceptor block. Bond length change is well-distributed along each block, indicating that there is good delocalization of the oxidized and reduced form within. A solution to the poor charge delocalization of alternating donor–acceptor copolymers might be the use of a block copolymer, where each block acts independently to store positive and negative charge. This system is beyond the scope of the present study but provides guidance for future work in this field. Moreover, on the basis of the agreement between the modeled and experimental data for PDEQ and PDDDBT, computational chemistry appears to provide rational design principles for future organic energy-storage materials.

#### 4. CONCLUSIONS

Donor–acceptor polymers have the unique ability to hold both a positive and negative charge at relatively modest potentials. Incorporating equal concentrations of donor and acceptor units in the polymer backbone results in improved capacitance matching in the positive and negative electroactive potential ranges, which is imperative for high-performance and stable devices. Negative charges are poorly delocalized across the polymer backbone, but incorporating two adjacent acceptor groups improves negative charging stability and the ambipolar characteristic of the material. Ambipolar charging allows the polymer to be used as the sole charge storage material in a Type III supercapacitor with the advantage of having a higher operating voltage than typical p-type conjugated polymers. The high operating voltage translates into specific energy and power values much higher than the reference PEDOT Type I device. Improved ambipolar character of the polymer dramatically improves the stability of the device.

Future work to develop high-performance donor–acceptor polymers for supercapacitors may be directed at developing donor–acceptor block copolymers to achieve good delocalization under both positive and negative charging. The development of very low band gap materials with early oxidation and reduction potentials will also be important because they will display pseudocapacitance over a greater potential range that will increase the capacity of the device.

#### ■ ASSOCIATED CONTENT

##### Supporting Information

Physical data for the monomers and polymer films, DDDQ cyclic voltammetry, PEDOT supercapacitor cycle stability measurements, additional computational chemistry data, full Gaussian 09 citation. This material is available free of charge via the Internet at <http://pubs.acs.org>.

#### ■ AUTHOR INFORMATION

##### Corresponding Author

\*Phone: 416-946-0285. E-mail: dseferos@chem.utoronto.ca.

##### Present Address

<sup>§</sup>T.M.M.: Portland State University, Department of Chemistry, P.O. Box 751, Portland, OR, 97207.

##### Author Contributions

The manuscript was written through contributions of all authors. All authors have given approval to the final version of the manuscript.

##### Notes

The authors declare no competing financial interest.

#### ■ ACKNOWLEDGMENTS

This work was supported by the University of Toronto, NSERC, the CFI, and the Ontario Research Fund. D.S.S. is grateful to NSERC (for the award of Canada Research Chair), the Connaught Foundation (for the Innovation Award), and DuPont (for the Young Professor Grant). P.M.D. is grateful for an Ontario Graduate Scholarship and a Queen Elizabeth II Graduate Scholarship in Science and Technology.

#### ■ REFERENCES

- (1) Conway, B. E.; Birss, V.; Wojtowicz, J. The Role and Utilization of Pseudocapacitance for Energy Storage by Supercapacitors. *J. Power Sources* **1997**, *66*, 1–14.
- (2) Conway, B. E. *Electrochemical Supercapacitors*; Kluwer Academic/Plenum Publishers: New York, 1999.
- (3) Simon, P.; Gogotsi, Y. Materials for Electrochemical Capacitors. *Nat. Mater.* **2008**, *7*, 845–854.
- (4) Wang, Y.; Xia, Y. Recent Progress in Supercapacitors: From Materials Design to System Construction. *Adv. Mater.* **2013**, *25*, 5336–5342.
- (5) Lee, K. T.; Ji, X.; Rault, M.; Nazar, L. F. Simple Synthesis of Graphitic Ordered Mesoporous Carbon Materials by a Solid-State Method Using Metal Phthalocyanines. *Angew. Chem., Int. Ed.* **2009**, *48*, 5661–5665.
- (6) Kim, A.; Black, R.; Hyun, Y. J.; Nazar, L. F.; Prouzet, E. Synthesis of Monolithic Meso–Macroporous Silica and Carbon with Tunable Pore Size. *Chem. Commun.* **2012**, *48*, 4335–4337.
- (7) Izadi-Najafabadi, A.; Yasuda, S.; Kobashi, K.; Yamada, T.; Futaba, D. N.; Hatori, H.; Yumura, M.; Iijima, S.; Hata, K. Extracting the Full Potential of Single-Walled Carbon Nanotubes as Durable Supercapacitor Electrodes Operable at 4 V with High Power and Energy Density. *Adv. Mater.* **2010**, *22*, E235–E241.
- (8) Lee, J. A.; Shin, M. K.; Kim, S. H.; Cho, H. U.; Spinks, G. M.; Wallace, G. G.; Lima, M. D.; Lepró, X.; Kozlov, M. E.; Baughman, R. H. Ultrafast Charge and Discharge Biscrolled Yarn Supercapacitors for Textiles and Microdevices. *Nat. Commun.* **2013**, *4*, 1970.
- (9) El-Kady, M. F.; Strong, V.; Dubin, S.; Kaner, R. B. Laser Scribing of High-Performance and Flexible Graphene-Based Electrochemical Capacitors. *Science* **2012**, *335*, 1326–1330.
- (10) Beidaghi, M.; Wang, C. Micro-Supercapacitors Based on Interdigital Electrodes of Reduced Graphene Oxide and Carbon Nanotube Composites with Ultrahigh Power Handling Performance. *Adv. Funct. Mater.* **2012**, *22*, 4501–4510.
- (11) Lee, J. W.; Hall, A. S.; Kim, J.-D.; Mallouk, T. E. A Facile and Template-Free Hydrothermal Synthesis of Mn<sub>3</sub>O<sub>4</sub> Nanorods on Graphene Sheets for Supercapacitor Electrodes with Long Cycle Stability. *Chem. Mater.* **2012**, *24*, 1158–1164.
- (12) El-Kady, M. F.; Kaner, R. B. Scalable Fabrication of High-Power Graphene Micro-Supercapacitors for Flexible and on-Chip Energy Storage. *Nat. Commun.* **2013**, *4*, 1475–1479.
- (13) Li, Y.; Li, Z.; Shen, P. K. Simultaneous Formation of Ultrahigh Surface Area and Three-Dimensional Hierarchical Porous Graphene-

- Like Networks for Fast and Highly Stable Supercapacitors. *Adv. Mater.* **2013**, *25*, 2474–2480.
- (14) Maxwell Technologies. [www.Maxwell.com](http://www.Maxwell.com).
- (15) Nescapp Ultracapitors. [www.Nescap.com](http://www.Nescap.com).
- (16) Ulgut, B.; Grose, J. E.; Kiya, Y.; Ralph, D. C.; Abruna, H. D. A New Interpretation of Electrochemical Impedance Spectroscopy to Measure Accurate Doping Levels for Conducting Polymers: Separating Faradaic and Capacitive Currents. *Appl. Surf. Sci.* **2009**, *256*, 1304–1308.
- (17) Roncali, J. Conjugated Poly (Thiophenes): Synthesis, Functionalization, and Applications. *Chem. Rev.* **1992**, *92*, 711–738.
- (18) Roncali, J. Electrogenerated Functional Conjugated Polymers as Advanced Electrode Materials. *J. Mater. Chem.* **1999**, *9*, 1875–1893.
- (19) *Handbook of Conducting Polymers*, 3rd ed.; Skotheim, T. A., Reynolds, J., Eds.; CRC Press: Boca Raton, FL, 2007.
- (20) Ertas, M.; Walczak, R. M.; Das, R. K.; Rinzler, A. G.; Reynolds, J. R. Supercapacitors Based on Polymeric Dioxyppyrroles and Single Walled Carbon Nanotubes. *Chem. Mater.* **2012**, *24*, 433–443.
- (21) Xu, Y.; Schwab, M. G.; Strudwick, A. J.; Hennig, I.; Feng, X.; Wu, Z.; Müllen, K. Screen-Printable Thin Film Supercapacitor Device Utilizing Graphene/Polyaniline Inks. *Adv. Energy Mater.* **2013**, *3*, 1035–1040.
- (22) Lowe, M. A.; Kiya, Y.; Henderson, J. C.; Abruna, H. D. Pendant Thioether Polymer for Redox Capacitor Cathodes. *Electrochim. Commun.* **2011**, *13*, 462–465.
- (23) Burkhardt, S. E.; Lowe, M. A.; Conte, S.; Zhou, W.; Qian, H.; Rodríguez-Calero, G. G.; Gao, J.; Hennig, R. G.; Abruna, H. D. Tailored Redox Functionality of Small Organics for Pseudocapacitive Electrodes. *Energy Environ. Sci.* **2012**, *5*, 7176–7187.
- (24) Cao, Y.; Mallouk, T. E. Morphology of Template-Grown Polyaniline Nanowires and Its Effect on the Electrochemical Capacitance of Nanowire Arrays. *Chem. Mater.* **2008**, *20*, 5260–5265.
- (25) Liu, R.; Cho, S. I.; Lee, S. B. Poly(3,4-Ethylenedioxythiophene) Nanotubes as Electrode Materials for a High-Powered Supercapacitor. *Nanotechnology* **2008**, *19*, 215710.
- (26) DiCarmine, P. M.; Fokina, A.; Seferos, D. S. Solvent/Electrolyte Control of the Wall Thickness of Template-Synthesized Nanostructures. *Chem. Mater.* **2011**, *23*, 3787–3794.
- (27) Huesmann, D.; DiCarmine, P. M.; Seferos, D. S. Template-Synthesized Nanostructure Morphology Influenced by Building Block Structure. *J. Mater. Chem.* **2011**, *21*, 408–413.
- (28) Duay, J.; Gillette, E.; Hu, J.; Lee, S. B. Controlled Electrochemical Deposition and Transformation of Hetero-Nanoarchitected Electrodes for Energy Storage. *Phys. Chem. Chem. Phys.* **2013**, *15*, 7976–7993.
- (29) Kowalski, D.; Albu, S. P.; Schmuki, P. Current Dependent Formation of PEDOT Inverse Nanotube Arrays. *RSC Adv.* **2013**, *3*, 2154–2157.
- (30) Havinga, E. E.; ten Hoeve, W.; Wynberg, H. A New Class of Small Band Gap Organic Polymer Conductors. *Polym. Bull.* **1992**, *29*, 119–126.
- (31) Havinga, E. E.; ten Hoeve, W.; Wynberg, H. Alternate Donor-Acceptor Small-Band-Gap Semiconducting Polymers; Polysquaraines and Polycroconaines. *Synth. Met.* **1993**, *55*, 299–306.
- (32) Jenekhe, S. A.; Lu, L.; Alam, M. M. New Conjugated Polymers with Donor–Acceptor Architectures: Synthesis and Photophysics of Carbazole–Quinoline and Phenothiazine–Quinoline Copolymers and Oligomers Exhibiting Large Intramolecular Charge Transfer. *Macromolecules* **2001**, *34*, 7315–7324.
- (33) Bundgaard, E.; Krebs, F. C. Low-Band-Gap Conjugated Polymers Based on Thiophene, Benzothiadiazole, and Benzobis-(Thiadiazole). *Macromolecules* **2006**, *39*, 2823–2831.
- (34) Gibson, G. L.; McCormick, T. M.; Seferos, D. S. Atomistic Band Gap Engineering in Donor-Acceptor Polymers. *J. Am. Chem. Soc.* **2012**, *134*, 539–547.
- (35) Guo, X.; Watson, M. D. Pyromellitic Diimide-Based Donor-Acceptor Poly(Phenylene Ethynylene)s. *Macromolecules* **2011**, *44*, 6711–6716.
- (36) Öktem, G.; Balan, A.; Baran, D.; Toppore, L. Donor–Acceptor Type Random Copolymers for Full Visible Light Absorption. *Chem. Commun.* **2011**, *47*, 3933–3935.
- (37) Jellison, J. L.; Lee, C.-H.; Zhu, X.; Wood, J. D.; Plunkett, K. N. Electron Acceptors Based on an All-Carbon Donor-Acceptor Copolymer. *Angew. Chem., Int. Ed.* **2012**, *51*, 12321–12324.
- (38) Wood, J. D.; Jellison, J. L.; Finke, A. D.; Wang, L.; Plunkett, K. N. Electron Acceptors Based on Functionalizable Cyclopenta[hi]-aceanthrylenes and Dicyclopenta[de,mn]Tetracenes. *J. Am. Chem. Soc.* **2012**, *134*, 15783–15789.
- (39) Fu, B.; Baltazar, J.; Hu, Z.; Chien, A.-T.; Kumar, S.; Henderson, C. L.; Collard, D. M.; Reichmanis, E. High Charge Carrier Mobility, Low Band Gap Donor–Acceptor Benzothiadiazole-Oligothiophene Based Polymeric Semiconductors. *Chem. Mater.* **2012**, *24*, 4123–4133.
- (40) Gibson, G. L.; McCormick, T. M.; Seferos, D. S. Effect of Group-14 and Group-16 Substitution on the Photophysics of Structurally Related Donor–Acceptor Polymers. *J. Phys. Chem. C* **2013**, *117*, 16606–16615.
- (41) McCormick, T. M.; Bridges, C. R.; Carrera, E. I.; DiCarmine, P. M.; Gibson, G. L.; Hollinger, J.; Kozyz, L. M.; Seferos, D. S. Conjugated Polymers: Evaluating DFT Methods for More Accurate Orbital Energy Modeling. *Macromolecules* **2013**, *46*, 3879–3886.
- (42) Kanal, I. Y.; Owens, S. G.; Bechtel, J. S.; Hutchison, G. R. Efficient Computational Screening of Organic Polymer Photovoltaics. *J. Phys. Chem. Lett.* **2013**, *4*, 1613–1623.
- (43) Norris, B. N.; Zhang, S.; Campbell, C. M.; Auletta, J. T.; Calvo-Marzal, P.; Hutchison, G. R.; Meyer, T. Y. Sequence Matters: Modulating Electronic and Optical Properties of Conjugated Oligomers via Tailored Sequence. *Macromolecules* **2013**, *46*, 1384–1392.
- (44) Worch, J. C.; Chirdon, D. N.; Maurer, A. B.; Qiu, Y.; Geib, S. J.; Bernhard, S.; Noonan, K. J. T. Synthetic Tuning of Electronic and Photophysical Properties of 2-Aryl-1,3-Benzothiaphospholes. *J. Org. Chem.* **2013**, *78*, 7462–7469.
- (45) Sonmez, G.; Shen, C. K. F.; Rubin, Y.; Wudl, F. A Red, Green, and Blue (RGB) Polymeric Electrochromic Device (PECD): the Dawning of the PECD Era. *Angew. Chem.* **2004**, *116*, 1524–1528.
- (46) Zhang, M.; Tsao, H. N.; Pisula, W.; Yang, C.; Mishra, A. K.; Müllen, K. Field-Effect Transistors Based on a Benzothiadiazole–Cyclopentadithiophene Copolymer. *J. Am. Chem. Soc.* **2007**, *129*, 3472–3473.
- (47) Zhou, E.; Nakamura, M.; Nishizawa, T.; Zhang, Y.; Wei, Q.; Tajima, K.; Yang, C.; Hashimoto, K. Synthesis and Photovoltaic Properties of a Novel Low Band Gap Polymer Based on N-Substituted Dithieno[3,2-b:2',3'-d]Pyrrole. *Macromolecules* **2008**, *41*, 8302–8305.
- (48) Tao, Y.; McCulloch, B.; Kim, S.; Segalman, R. A. The Relationship Between Morphology and Performance of Donor–Acceptor Rod–Coil Block Copolymer Solar Cells. *Soft Matter* **2009**, *5*, 4219–4230.
- (49) Beaujuge, P. M.; Amb, C. M.; Reynolds, J. R. Spectral Engineering in  $\Pi$ -Conjugated Polymers with Intramolecular Donor–Acceptor Interactions. *Acc. Chem. Res.* **2010**, *43*, 1396–1407.
- (50) Hains, A. W.; Liang, Z.; Woodhouse, M. A.; Gregg, B. A. Molecular Semiconductors in Organic Photovoltaic Cells. *Chem. Rev.* **2010**, *110*, 6689–6735.
- (51) Burkhardt, B.; Khlyabich, P. P.; Canak, T. C.; LaJoie, T. W.; Thompson, B. C. Semi-Random” Multichromophoric rr-P3HT Analogues for Solar Photon Harvesting. *Macromolecules* **2011**, *44*, 1242–1246.
- (52) Evenson, S. J.; Mumm, M. J.; Pokhodnya, K. I.; Rasmussen, S. C. Highly Fluorescent Dithieno[3,2-b:2',3'-d]Pyrrole-Based Materials: Synthesis, Characterization, and OLED Device Applications. *Macromolecules* **2011**, *44*, 835–841.
- (53) Rasmussen, S. C.; Schwiderski, R. L.; Mulholland, M. E. Thieno[3,4-b]pyrazines and Their Applications to Low Band Gap Organic Materials. *Chem. Commun.* **2011**, *47*, 11394–11410.
- (54) Wang, E.; Ma, Z.; Zhang, Z.; Vandewal, K.; Henriksson, P.; Inganäs, O.; Zhang, F.; Andersson, M. R. An Easily Accessible

- Isoindigo-Based Polymer for High-Performance Polymer Solar Cells. *J. Am. Chem. Soc.* **2011**, *133*, 14244–14247.
- (55) Sista, P.; Kularatne, R. S.; Mulholland, M. E.; Wilson, M.; Holmes, N.; Zhou, X.; Dastoor, P. C.; Belcher, W.; Rasmussen, S. C.; Biewer, M. C.; et al. Synthesis and Photovoltaic Performance of Donor-Acceptor Polymers Containing Benzo[1,2-*b*:4,5-*b'*]dithiophene with Thienyl Substituents. *J. Polym. Sci., Polym. Chem.* **2013**, *51*, 2622–2630.
- (56) Rudge, A.; Davey, J.; Raistrick, I.; Gottesfeld, S.; Ferraris, J. P. Conducting Polymers as Active Materials in Electrochemical Capacitors. *J. Power Sources* **1994**, *47*, 89–107.
- (57) Rudge, A.; Raistrick, I.; Gottesfeld, S.; Ferraris, J. P. A Study of the Electrochemical Properties of Conducting Polymers for Application in Electrochemical Capacitors. *Electrochim. Acta* **1994**, *39*, 273–287.
- (58) Ferraris, J. P.; Eissa, M. M.; Brotherston, I. D.; Loveday, D. C. Performance Evaluation of Poly 3-(Phenylthiophene) Derivatives as Active Materials for Electrochemical Capacitor Applications. *Chem. Mater.* **1998**, *10*, 3528–3535.
- (59) Fusalba, F.; El Mehdi, N.; Breau, L.; Bélanger, D. Physicochemical and Electrochemical Characterization of Polycyclopenta[2,1-*b*;3,4-*b'*]dithiophen-4-one as an Active Electrode for Electrochemical Supercapacitors. *Chem. Mater.* **1999**, *11*, 2743–2753.
- (60) Mastragostino, M.; Arbizzani, C.; Paraventi, R.; Zanelli, A. Polymer Selection and Cell Design for Electric-Vehicle Supercapacitors. *J. Electrochem. Soc.* **2000**, *147*, 407–412.
- (61) Fusalba, F.; Ho, H. A.; Breau, L.; Bélanger, D. Poly(Cyano-Substituted Diheteroareneethylene) as Active Electrode Material for Electrochemical Supercapacitors. *Chem. Mater.* **2000**, *12*, 2581–2589.
- (62) Soudan, P.; Ho, H. A.; Breau, L.; Bélanger, D. Chemical Synthesis and Electrochemical Properties of Poly(Cyano-Substituted-Diheteroareneethylene) as Conducting Polymers for Electrochemical Supercapacitors. *J. Electrochem. Soc.* **2001**, *148*, A775–A782.
- (63) Soudan, P.; Lucas, P.; Ho, H. A.; Jobin, D.; Breau, L.; Bélanger, D. Synthesis, Chemical Polymerization and Electrochemical Properties of Low Band Gap Conducting Polymers for Use in Supercapacitors. *J. Mater. Chem.* **2001**, *11*, 773–782.
- (64) Estrada, L. A.; Liu, D. Y.; Salazar, D. H.; Dyer, A. L.; Reynolds, J. R. Poly[Bis-EDOT-Isoindigo]: an Electroactive Polymer Applied to Electrochemical Supercapacitors. *Macromolecules* **2012**, *45*, 8211–8220.
- (65) DuBois, C. J.; Reynolds, J. R. 3,4-Ethylenedioxothiophene-Pyridine-Based Polymers: Redox or n-Type Electronic Conductivity? *Adv. Mater.* **2002**, *14*, 1844–1846.
- (66) Zhu, S. S.; Swager, T. M. Conducting Polymetalloroxanes: Metal Ion Mediated Enhancements in Conductivity and Charge Localization. *J. Am. Chem. Soc.* **1997**, *119*, 12568–12577.
- (67) Durmus, A.; Gunbas, G. E.; Toppare, L. New, Highly Stable Electrochromic Polymers From 3, 4-Ethylenedioxothiophene–Bis-Substituted Quinoxalines Toward Green Polymeric Materials. *Chem. Mater.* **2007**, *19*, 6247–6251.
- (68) Mohanakrishnan, A. K.; Hucke, A.; Lyon, M. A.; Lakshminathan, M. V.; Cava, M. P. Functionalization of 3,4-Ethylenedioxothiophene. *Tetrahedron* **1999**, *55*, 11745–11754.
- (69) Reichart, B.; Kappe, C. O. High-Temperature Continuous Flow Synthesis of 1,3,4-Oxadiazoles via N-Acylation of 5-Substituted Tetrazoles. *Tetrahedron Lett.* **2012**, *53*, 952–955.
- (70) Becke, A. D. Density-Functional Thermochemistry. III. The Role of Exact Exchange. *J. Chem. Phys.* **1993**, *98*, 5648–5652.
- (71) Yanai, T.; Tew, D. P.; Handy, N. C. A New Hybrid Exchange–Correlation Functional Using the Coulomb-Attenuating Method (CAM-B3LYP). *Chem. Phys. Lett.* **2004**, *393*, 51–57.
- (72) Frisch, M. J.; et al. Gaussian 09, revision B.01; Gaussian, Inc.: Wallingford, CT, 2009.
- (73) Dennington, R.; Keith, T.; Millam, J. *GaussView*, version 5; Semichem, Inc.: Shawnee Mission, KS, 2009.
- (74) DuBois, C. J.; Abboud, K. A.; Reynolds, J. R. Electrolyte-Controlled Redox Conductivity and n-Type Doping in Poly(bis-EDOT-Pyridine)s. *J. Phys. Chem. B* **2004**, *108*, 8550–8557.
- (75) Gunbas, G. E.; Durmus, A.; Toppare, L. Could Green Be Greener? Novel Donor–Acceptor-Type Electrochromic Polymers: Towards Excellent Neutral Green Materials with Exceptional Transmissive Oxidized States for Completion of RGB Color Space. *Adv. Mater.* **2008**, *20*, 691–695.
- (76) Pamuk, M.; Tirkes, S.; Cihaner, A.; Algi, F. A New Low-Voltage-Driven Polymeric Electrochromic. *Polymer* **2010**, *51*, 62–68.
- (77) Matsidik, R.; Mamtimin, X.; Mi, H. Y.; Nurulla, I. Synthesis and Properties of Polymer From bis-3,4-Ethylenedioxothiophene Substituted Acenaphthenequinoxaline. *J. Appl. Polym. Sci.* **2010**, *118*, 74–80.
- (78) Tarkuc, S.; Uduum, Y. A.; Toppare, L. Molecular Architecture: Another Plausible Pathway Toward a Low Band Gap Polymer. *J. Electroanal. Chem.* **2010**, *643*, 89–93.
- (79) Tarkuc, S.; Unver, E. K.; Uduum, Y. A.; Toppare, L. Multi-Colored Electrochromic Polymer with Enhanced Optical Contrast. *Eur. Polym. J.* **2010**, *46*, 2199–2205.
- (80) Beaujuge, P. M.; Subbiah, J.; Choudhury, K. R.; Ellinger, S.; McCarley, T. D.; So, F.; Reynolds, J. R. Green Dioxythiophene-Benzothiadiazole Donor–Acceptor Copolymers for Photovoltaic Device Applications. *Chem. Mater.* **2010**, *22*, 2093–2106.
- (81) Lin, Y.; Cheng, P.; Liu, Y.; Shi, Q.; Hu, W.; Li, Y.; Zhan, X. Small Molecules Based on Bithiazole for Solution-Processed Organic Solar Cells. *Org. Electron.* **2012**, *13*, 673–680.
- (82) Yassin, A.; Savitha, G.; Leriche, P.; Frère, P.; Roncali, J. A Donor–Acceptor–Donor (D–A–D) Molecule Based on 3-Alkoxy-4-Cyanothiophene and Dithienopyrrole Units as Active Material for Organic Solar Cells. *New J. Chem.* **2012**, *36*, 2412–2416.
- (83) Yassin, A.; Leriche, P.; Allain, M.; Roncali, J. Donor–Acceptor–Donor (D–A–D) Molecules Based on Isoindigo as Active Material for Organic Solar Cells. *New J. Chem.* **2013**, *37*, 502–507.
- (84) Cai, Z.; Guo, Y.; Yang, S.; Peng, Q.; Luo, H.; Liu, Z.; Zhang, G.; Liu, Y.; Zhang, D. New Donor–Acceptor–Donor Molecules with Pechmann Dye as the Core Moiety for Solution-Processed Good-Performance Organic Field-Effect Transistors. *Chem. Mater.* **2013**, *25*, 471–478.
- (85) Aydar, S.; Böyükayram, A. E.; Sendur, M.; Toppare, L. Immobilization of Invertase in DAD Type Polymers: Combination of Benzothiadiazole Acceptor Unit and 3,4-Ethylenedioxothiophene and Thiophene Donor Units. *J. Macromol. Sci., Part A* **2011**, *48*, 855–861.
- (86) Schipper, D. J.; Fagnou, K. Direct Arylation as a Synthetic Tool for the Synthesis of Thiophene-Based Organic Electronic Materials. *Chem. Mater.* **2011**, *23*, 1594–1600.
- (87) Kowalski, S.; Allard, S.; Zilberberg, K.; Riedl, T.; Scherf, U. Direct Arylation Polycondensation as Simplified Alternative for the Synthesis of Conjugated (Co)Polymers. *Prog. Polym. Sci.* **2013**, *38*, 1805–1814.
- (88) Mercier, L. G.; Leclerc, M. Direct (Hetero)Arylation: a New Tool for Polymer Chemists. *Acc. Chem. Res.* **2013**, *46*, 1597–1605.
- (89) Fuller, A. A.; Hester, H. R.; Salo, E. V.; Stevens, E. P. In Situ Formation and Reaction of 2-Pyridylboronic Esters. *Tetrahedron Lett.* **2003**, *44*, 2935–2938.
- (90) Heinze, J.; Frontana-Uribe, B. A.; Ludwigs, S. Electrochemistry of Conducting Polymers—Persistent Models and New Concepts. *Chem. Rev.* **2010**, *110*, 4724–4771.
- (91) Janietz, S.; Schulz, B.; Törrönen, M.; Sundholm, G. Electrochemical Investigations on Poly(Phenylene-1,3,4-oxadiazoles). *Eur. Polym. J.* **1993**, *29*, 545–549.
- (92) Kress, L.; Neudeck, A.; Petr, A.; Dunsch, L. In Situ Spectroelectrochemistry of 2,5-Diphenyl-1,3,4-oxadiazole. *J. Electroanal. Chem.* **1996**, *414*, 31–40.
- (93) Stoller, M. D.; Ruoff, R. S. Best Practice Methods for Determining an Electrode Material’s Performance for Ultracapacitors. *Energy Environ. Sci.* **2010**, *3*, 1294–1301.
- (94) Razaq, A.; Nyholm, L.; Sjödin, M.; Strømme, M.; Mihranyan, A. Paper-Based Energy-Storage Devices Comprising Carbon Fiber-

Reinforced Polypyrrole-Cladophora Nanocellulose Composite Electrodes. *Adv. Energy Mater.* **2012**, *2*, 445–454.

(95) Jha, N.; Ramesh, P.; Bekyarova, E.; Itkis, M. E.; Haddon, R. C. High Energy Density Supercapacitor Based on a Hybrid Carbon Nanotube—Reduced Graphite Oxide Architecture. *Adv. Energy Mater.* **2012**, *2*, 438–444.

(96) Xiong, G.; Meng, C.; Reifenberger, R. G.; Irazoqui, P. P.; Fisher, T. S. Graphitic Petal Electrodes for All-Solid-State Flexible Supercapacitors. *Adv. Energy Mater.* **2013**, *4*, 1300515.

(97) Kim, H.; Cho, M. Y.; Kim, M. H.; Park, K. Y. A Novel High-Energy Hybrid Supercapacitor with an Anatase TiO<sub>2</sub>—Reduced Graphene Oxide Anode and an Activated Carbon Cathode. *Adv. Energy Mater.* **2013**, *3*, 1500–1506.

(98) Zotti, G.; Zecchin, S.; Schiavon, G.; Groenendaal, L. B. Conductive and Magnetic Properties of 3,4-Dimethoxy- and 3,4-Ethylenedioxy-Capped Polypyrrole and Polythiophene. *Chem. Mater.* **2000**, *12*, 2996–3005.

(99) Szkurlat, A.; Palys, B.; Mieczkowski, J.; Skompska, M. Electrosynthesis and Spectroelectrochemical Characterization of Poly(3,4-Dimethoxy-thiophene), Poly(3,4-Dipropoxythiophene) and Poly(3,4-Dioctyloxythiophene) Films. *Electrochim. Acta* **2003**, *48*, 3665–3676.

(100) Jeon, J.-W.; Ma, Y.; Mike, J. F.; Shao, L.; Balbuena, P. B.; Lutkenhaus, J. L. Oxidatively Stable Polyaniline: Polyacid Electrodes for Electrochemical Energy Storage. *Phys. Chem. Chem. Phys.* **2013**, *15*, 9654–9662.

(101) Becke, A. D. Density-Functional Thermochemistry. I. The Effect of the Exchange-Only Gradient Correction. *J. Chem. Phys.* **1992**, *96*, 2155–2160.